AAC
Journals.ASM.org

Pharmacokinetics and Pharmacodynamics of Anidulafungin for Experimental *Candida* Endophthalmitis: Insights into the Utility of Echinocandins for Treatment of a Potentially Sight-Threatening Infection

J. L. Livermore,[a,b] T. W. Felton,[a] J. Abbott,[c] A. Sharp,[a,b] J. Goodwin,[a,b] L. Gregson,[a,b] P. A. Warn,[a] S. J. Howard,[a,b] W. W. Hope[a,b]

The University of Manchester, Manchester Academic Health Science Centre, NIHR Translational Research Facility in Respiratory Medicine, University Hospital of South Manchester NHS Foundation Trust, Manchester, United Kingdom[a]; Department of Molecular and Clinical Pharmacology, University of Liverpool, Liverpool, United Kingdom[b]; Birmingham Children's Hospital, Birmingham, United Kingdom[c]

***Candida* chorioretinitis and endophthalmitis are relatively common manifestations of disseminated candidiasis. Anidulafungin is increasingly used for the treatment of disseminated candidiasis, but its efficacy for *Candida* endophthalmitis is not known. A nonneutropenic model of hematogenous *Candida* endophthalmitis was used. Anidulafungin at 5, 10, and 20 mg/kg was initiated at 48 h postinoculation. The fungal densities in the kidney and vitreous humor were determined. Anidulafungin concentrations in the plasma and vitreous humor were measured using high-performance liquid chromatography (HPLC). A pharmacokinetic-pharmacodynamic model was used to link anidulafungin concentrations with the observed antifungal effect. The area under the concentration-time curve (AUC) associated with stasis was determined in the both the kidney and the vitreous humor. The results were bridged to humans to identify likely dosages that are associated with significant antifungal activity within the eye. Inoculation of *Candida albicans* resulted in logarithmic growth in both the vitreous humor and the kidney. The pharmacokinetics of anidulafungin were linear. There was dose-dependent penetration of the anidulafungin into the vitreous humor. The exposure-response relationships in the kidney and vitreous were completely discordant. AUCs of 270 and 100 were required for stasis in the eye and kidney, respectively. The currently licensed regimen results in an AUC for an average patient that is associated with stasis in the kidney but minimal antifungal activity in the eye. We conclude that anidulafungin penetrates the eye in a dose-dependent manner and that dosages higher than those currently licensed are required to achieve significant antifungal activity in the eye.**

Candida endophthalmitis is a potentially sight-threatening infection that is difficult to treat and can affect any age group (1–4). A schematic depiction of this syndrome is shown in Fig. 1. Endogenous ocular syndromes caused by *Candida* spp. range from infection limited to chorioretinal structures through to involvement of the entire globe. The estimated incidence of endogenous *Candida* endophthalmitis varies tremendously (5–7). The most common causative fungal pathogen is *Candida albicans*, although a range of *Candida* species have also been documented (5). Despite being described over 70 years ago, the optimal treatment for *Candida* endophthalmitis is unknown.

A number of systemic antifungal agents are available for treatment of *Candida* endophthalmitis, including the triazoles and the polyenes (8). The role of the echinocandins is less certain. The evidence that supports the use of various antifungal agents has been accrued over many years from case reports (see, for example, reference 9) and case series (10); there are no randomized clinical trials. The Infectious Diseases Society of America (IDSA) guidelines for the treatment of endogenous *Candida* endophthalmitis recommend intravenous amphotericin B deoxycholate at 0.7 to 1 mg/kg daily with or without oral flucytosine at 25 mg/kg every 6 h (8). Adjunctive therapies include vitrectomy with intravitreal injection of antifungal agents. These additional measures may be required if there is extensive vitreal disease and if there are concerns that poor ocular penetration of antifungal compounds may compromise the antifungal effect and the clinical outcome.

The echinocandins are increasingly considered first-line agents for the treatment of candidemia and invasive candidiasis (8). Anidulafungin is a semisynthetic lipopeptide derived from *Aspergillus nidulans* (11). Based on the results of a randomized clinical trial, this agent is approved in the United States and Europe for the treatment of invasive candidiasis and candidemia (12). Because *Candida* endophthalmitis can result in devastating visual loss, further information is required to further understand the exposure-response relationships of newer antifungal agents for intraocular infections. Here, we used a rabbit model of endogenous *Candida* endophthalmitis to define the pharmacokinetics and pharmacodynamic relationships for anidulafungin against *Candida* endophthalmitis and then bridged these results to humans.

(This work was presented, in part, at the 22nd European Congress of Clinical Microbiology and Infectious Diseases [ECCMID]), London, United Kingdom, 2012.)

Received 6 July 2012 **Returned for modification** 4 August 2012
Accepted 20 October 2012
Published ahead of print 31 October 2012
Address correspondence to W. W. Hope, william.hope@liverpool.ac.uk.

doi:10.1128/AAC.01387-12

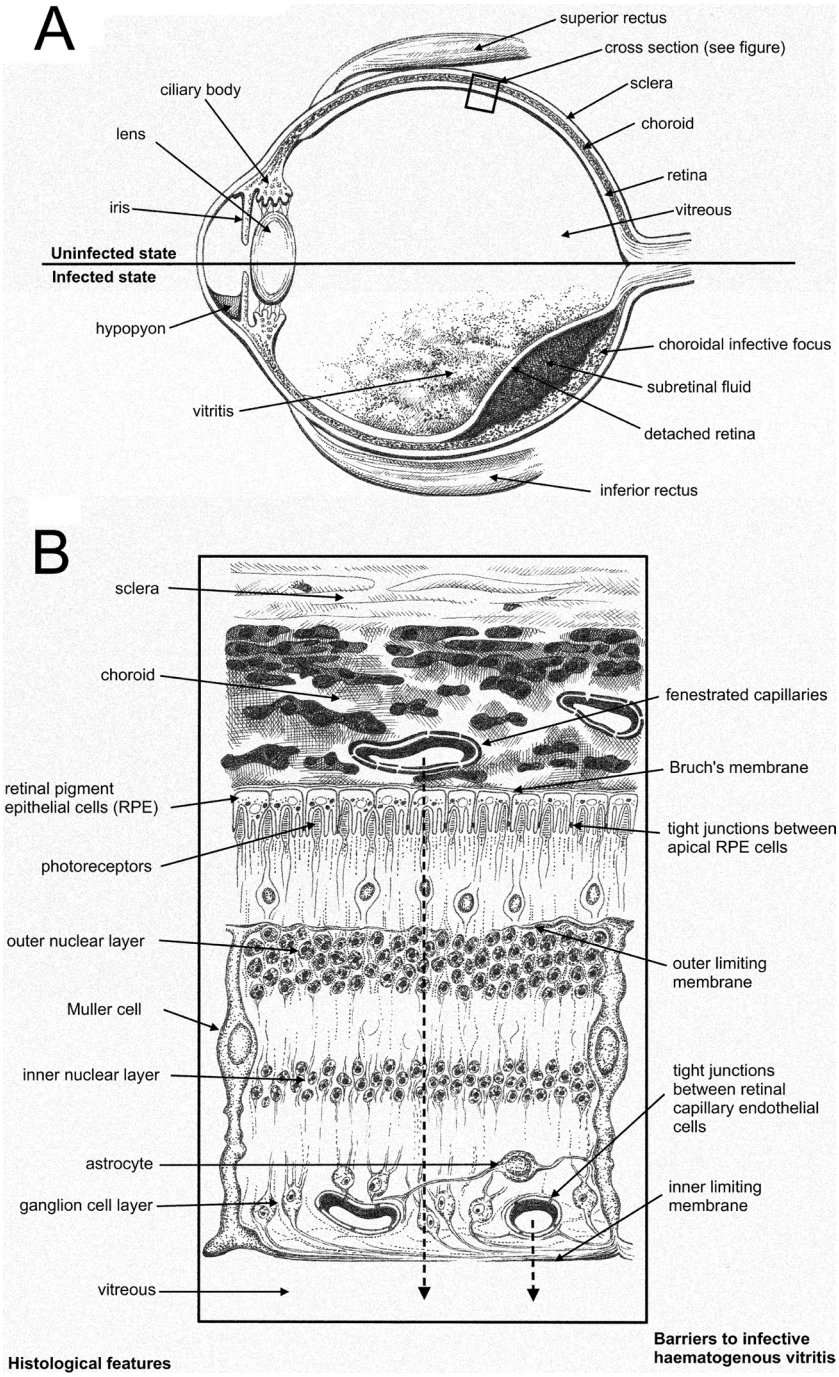

FIG 1 Schematic representation of the pathogenesis of *Candida* chorioretinitis and *Candida* endophthalmitis. (A) Sagittal section of the globe showing normal structures (upper half) and pathological features of *Candida* endophthalmitis (bottom half). (B) Schematic representation of the microscopic cross section through the eye. The course of infection from the choroid through to the vitreous is shown by the broken arrows.

MATERIALS AND METHODS

Rabbits. All experiments were conducted under Home Office project license PPL40/3101 and approved by The University of Manchester's ethics committee. A previously described and well-validated rabbit model of central nervous system candidiasis and endophthalmitis was used (13–16). Male New Zealand White rabbits weighing 2 to 3 kg were used for all experiments. As previously described, a subcutaneous intravenous port (Titanium Soloports; Linton Instrumentation, Norfolk, United Kingdom) was used to allow repeated atraumatic venous access for inoculum administration, drug administration, and procurement of plasma samples (16). Central venous access was established under general anesthesia and was performed by Harlan Laboratories UK, Ltd. The line was flushed with 1 ml of 0.9% saline followed by 0.5 ml of wash solution (0.1 ml sodium heparin [5,000 U/liter] plus 9.9 ml 0.9% normal saline) and then locked with 0.1 ml lock solution (9 ml 5% dextrose with 1 ml sodium heparin [5,000 U/ml]) immediately after use.

Challenge strain. The challenge strain was ATCC MYA1237 (NIH 8621), as has been used previously in this model (13, 14, 16). The MIC for the challenge strain was 0.0039 mg/liter using both CLSI and EUCAST methodologies. *Candida albicans* was retrieved from beads stored at −80°C, plated onto Sabouraud agar (Oxoid, United Kingdom), and then incubated at 37°C for 24 h. Several colonies were placed in Sabouraud broth. The desired inoculum (10^6 organisms) was based on previous studies of *Candida* meningoencephalitis (13, 14, 16) and was designed to induce reproducible infection within the central nervous system and eye. The inoculum was prepared using a hemocytometer and administered as a bolus in 1 ml of phosphate-buffered saline (PBS). Food and water were provided to rabbits *ad libitum*.

Pharmacokinetic and pharmacodynamic studies. The experimental period lasted for 4 days because of death of all control rabbits by 96 hours postinfection. Mortality appeared to occur as a result of significant neurological events, including seizures, rather than uncontrolled sepsis. Rabbits were sacrificed at predefined time points throughout the experiment or if neurological symptoms prevented access to food and water. Terminal pharmacokinetic and pharmacodynamics samples were obtained from all rabbits. Rabbits were sacrificed using a lethal dose of intravenous (i.v.) pentobarbital (80 mg/kg; Animalcare, Ltd., York, United Kingdom), which was administered via the indwelling catheter.

The clinical formulation of anidulafungin was reconstituted in sterile water and further diluted to obtain the desired concentrations. Anidulafungin was administered at 48 hours postinfection, as has been previously described for this model (16). Anidulafungin was administered over 1 min via the indwelling catheter. Based on preliminary dose-finding studies, dosages of 5, 10, and 20 mg/kg were used. Rabbits in the treatment groups received anidulafungin once or twice at 48 and 72 h postinfection. Experiments were repeated multiple times using a total of 6 rabbits for any one experiment (two rabbits for each dosage) and the results pooled for analysis. The total population of rabbits ($n = 35$) used in these experiments was analyzed using a population methodology (see below).

Plasma was collected in the first and second dosing intervals at 0, 0.5, 1, 2, 6, and 24 h after administration of anidulafungin. Blood samples were placed on ice and then centrifuged for 3 min. Plasma was stored at −80°C until analysis. Immediately after sacrifice, the anterior chamber of each eye was pierced with a sterile 23-gauge needle, and 0.3 to 0.4 ml of total aqueous humor was removed. One hundred microliters of aqueous humor (neat) was plated onto Sabouraud agar. Subsequently, both eyes were dissected free from the orbit by cutting the extraocular muscles and the optic nerve. An incision was placed through the sclera and into the posterior chamber of the eye to enable vitreous humor to be collected using a 10-ml syringe. The vitreous humor was then homogenized. Serial 10-fold dilutions were prepared in PBS, which were then plated to Sabouraud agar. For some rabbits, the kidneys were also dissected. A 1-g portion was removed and homogenized in PBS, and serial dilutions prepared and plated. All Sabouraud agar plates were incubated at 37°C for 24 h, after which the colonies in the various tissue matrices were counted.

Measurement of anidulafungin in rabbit plasma and vitreous humor. Anidulafungin concentrations in rabbit plasma and vitreous humor were measured using high-performance liquid chromatography (HPLC) with a Shimadzu Prominence (Shimadzu, Milton Keynes, United Kingdom). A Kinetex 2.6-μm C_{18} New Column (75 by 4.6 mm) was used (Phenomenex, Macclesfield, United Kingdom). A 5-μl injection volume was used. A standard curve encompassing 0.05 to 10 mg/liter in plasma and 0.006 to 10 mg/liter in the remaining matrix was constructed from stock solutions of anidulafungin (1,000 mg/liter in dimethyl sulfoxide [DMSO]) further diluted in methanol (Fisher Scientific, Loughborough, United Kingdom). The internal standard was micafungin. The mobile phase was 65% 0.1% trifluoroacetic acid (TFA) in water–35% acetonitrile with 0.1% TFA (vol/vol) with a gradient profile changing to 30% and 70%, respectively, over 4 min, with an overall run time of 6.25 min and flow rate of 1 ml/min. Anidulafungin was detected using fluorescence with excitation at 273 nm and emission at 464 nm. Anidulafungin and the internal standard eluted after 3.4 and 4.5 min, respectively. For plasma, the coefficient of variation (CV) was <2.4% over the concentration range of 0.05 to 10 mg/liter. The limit of detection was 0.05 mg/liter. The intra- and interday variations were <2.4%. For the remaining matrix, the CV was <4.7% over the concentration range of 0.006 to 10 mg/liter. The limit of detection was 0.006 mg/liter. The intra- and interday variations were <5%.

Mathematical modeling. The pharmacokinetic and pharmacodynamic data were modeled using a population methodology. The population pharmacokinetic program Big nonparametric adaptive grid (Big NPAG) was used (17). The structural mathematical model consisted of five compartments, and a schematic representation is shown in Fig. 1. The differential equations that were used were as follows:

$$dX_1/dt = R(1) - (\mathrm{kcp} + \mathrm{kce} + \mathrm{SCL}/V_c) \times X_1 + \mathrm{kec} \times X_2 + \mathrm{kpc} \times X_3 \quad (1)$$

$$dX_2/dt = \mathrm{kce} \times X_1 - \mathrm{kec} \times X_2 \quad (2)$$

$$dX_3/dt = \mathrm{kcp} \times X_1 - \mathrm{kpc} \times X_3 \quad (3)$$

$$dN_{\mathrm{eye}}/dt = \mathrm{kgmax}_{\mathrm{eye}} \times [1 - (\mathrm{N}_{\mathrm{eye}}/\mathrm{POPMAX}_{\mathrm{eye}})] \times N_{\mathrm{eye}} \quad (4a)$$

$$\times \{1 - [(X_2/V_{\mathrm{eye}})^{\mathrm{Hg\text{-}eye}}/(X_2/V_{\mathrm{eye}})^{\mathrm{Hg\text{-}eye}} + (C_{50}g_{\mathrm{eye}}{}^{\mathrm{Hg\text{-}eye}})]\} \quad (4b)$$

$$- \mathrm{Kkmax}_{\mathrm{eye}} \times [(X_2/V_{\mathrm{eye}})^{\mathrm{Hk\text{-}eye}}/(X_2/V_{\mathrm{eye}})^{\mathrm{Hk\text{-}eye}} + (C_{50}k_{\mathrm{eye}}{}^{\mathrm{Hk\text{-}eye}})] \times N_{\mathrm{eye}} \quad (4c)$$

$$dN_{\mathrm{kidney}}/dt = Kg\mathrm{max}_{\mathrm{kidney}} \times [1 - (N_{\mathrm{kidney}}/\mathrm{POPMAX}_{\mathrm{kidney}})] \times N_{\mathrm{kidney}} \quad (5a)$$

$$\times \{1 - [(X_1/V_c)^{\mathrm{Hg\text{-}kidney}}/(X_1/V_c)^{\mathrm{Hg\text{-}kidney}} + (C_{50}g_{\mathrm{kidney}}{}^{\mathrm{Hg\text{-}kidney}})]\} \quad (5b)$$

$$- \mathrm{Kkmax}_{\mathrm{kidney}} \times [(X_1/V_c)^{\mathrm{Hk\text{-}kidney}}/(X_1/V_c)^{\mathrm{Hk\text{-}kidney}} + (C_{50}k_{\mathrm{kidney}}{}^{\mathrm{Hk\text{-}kidney}})] \times N_{\mathrm{kidney}} \quad (5c)$$

where X_1, X_2, and X_3 are the amounts of anidulafungin (in milligrams) in the central compartment (plasma), vitreous humor, and peripheral compartment, respectively; $R(1)$ represents the infusion of anidulafungin into the bloodstream via the central venous catheter; SCL is the clearance of anidulafungin from the central compartment; V_c and V_{eye} are the volumes of central compartment and vitreous humor, respectively; kcp, kpc, kce, and kec are the first-order rate constants that connect the respective compartments; N is the burden (organisms/gram vitreous humor or kidney) of *Candida albicans*; Kgmax is the maximal rate of growth in the vitreous humor or kidney; POPMAX is the theoretical maximal density within the vitreous humor or kidney; Hg is the slope function for the suppression of growth in the vitreous humor or kidney; $C_{50}g$ is the concentration of drug producing half-maximal suppression of growth; Kkmax is the maximal rate of kill in the vitreous humor or kidney; Hk is the slope functions for the fungal kill in the vitreous humor or kidney; and $C_{50}k$ is the concentration of drug in the vitreous humor or kidney where fungal kill is half maximal.

Equation 1 describes the rate of change of anidulafungin in the central compartment (plasma). Equation 2 describes the rate of change of drug in the vitreous humor. Equation 3 describes the rate of change of drug in the peripheral compartment (i.e., everything other than the blood and the vitreous humor). Equation 4 describes the rate of change of fungal burden in the vitreous humor and contains terms describing the capacity-limited growth of *Candida albicans* (equation 4a), the drug-associated suppression of growth in the eye (fungistatic term) (equation 4b), and the drug-associated fungal kill in the eye (fungicidal term) (equation 4c). Equation 5 describes the rate of change of fungal burden in the kidney and contains terms describing the capacity-limited growth of *Candida albicans* (equation 5a), the drug-associated suppression of growth in the kidney (fungistatic term) (equation 5b), and the drug-associated fungal kill in the kidney (fungicidal term) (equation 5c).

The weighting function for each output was determined using the maximum-likelihood estimator in ADAPT 5 (18), as previously described. The data from rabbits receiving the same anidulafungin regimen were pooled to estimate these values. The fit of the model to the data was assessed by mean weighted error (a measure of precision), by mean weighted squared error (a measure of bias), and by visual inspection and coefficient of determination (r^2) of the linear regression of the observed and predicted values both before and after the Bayesian step.

The area under the concentration-time curve (AUC) in both plasma and the vitreous humor was estimated from the mathematical model. The structural mathematical model was implemented within the simulation module of ADAPT 5 (18). The AUCs were estimated using integration.

Bridging from rabbits to humans. To further place the experimental findings in a clinical context, the experimental results were bridged from rabbits to humans. The area under the concentration-time curve (AUC) in the second dosing interval was used as a measure of drug exposure. The mathematical model (described above) was used to estimate the relationship between AUC and the antifungal effect in the vitreous humor and the kidney. The stasis line was defined as the fungal density in the respective tissues at the time treatment was commenced. The AUCs (mean ± standard deviation) for the results from anidulafungin therapy in neonates (3 mg/kg, followed by 1.5 mg/kg i.v.), children (3 mg/kg, followed by 1.5 mg/kg i.v.), and adults (200-mg load, then 100 mg/day i.v.) (obtained from references 19 and 16) were compared with the experimental AUCs achieved in rabbits, thus enabling a visual comparison of the likely antifungal effects of these regimens in different patient populations.

RESULTS

Following i.v. inoculation of *Candida albicans*, there was rapid hematogenous dissemination to the kidney and the vitreous humor (see Fig. 3). The estimates from the mathematical model for the median fungal densities in the kidney and the vitreous humor immediately following infection were 573 and 3 organisms/gram tissue, respectively (Table 1). Over the course of the experimental period, there was progressive logarithmic growth at both effect sites. The fungal densities in the vitreous humor and kidney at the time of the initiation of therapy (i.e., 48 h after inoculation) were 2.02 and 4.63 $\log_{10}$ CFU/g, respectively (these estimates were used to define the stasis line). The aqueous humor remained sterile throughout the experimental period in control animals (data not shown).

Anidulafungin was well tolerated, with no evidence of drug-related toxicity following the administration of 20 mg/kg infused i.v. over 1 min. The pharmacokinetics of anidulafungin were linear. Anidulafungin was detectable in the vitreous humor immediately following the first dose and thereafter. There was no evidence of progressive accumulation of anidulafungin within the vitreous humor. There was dose-dependent penetration of anidulafungin into the vitreous humor, and the concentration-time profiles in the plasma and eye had similar shapes (i.e., there was no evidence of hysteresis) (Fig. 2). The $AUC_{vitreous\ humor}/AUC_{plasma}$ ratio was 2.3%.

The pharmacodynamics of anidulafungin in the eye were somewhat variable, which is consistent with previously observed effects of antifungal agents in this rabbit model of central nervous system infection (13, 14, 16). The administration of anidulafungin at 5 mg/kg had a negligible effect on the fungal density in the vitreous humor. In contrast there was a small but definite effect on the fungal density in the kidney (Fig. 3B). There was a progressive antifungal effect within the vitreous humor following the administration of higher dosages. The administration of 20 mg/kg was required to achieve a fungistatic effect (i.e., to prevent progressive fungal growth from the time of drug administration) (Fig. 3D). In contrast, the administration of these higher dosages resulted in progressive fungicidal activity in the kidney (Fig. 3C and D), with a net decline in fungal density.

TABLE 1 Model parameter means, medians, and standard deviations

Parameter (units)[a]	Mean	Median	SD
SCL (liters/h)	0.191	0.208	0.048
V_c (liters)	0.825	0.789	0.261
kce (h^{-1})	5.328	0.381	8.562
kec (h^{-1})	5.251	0.265	7.528
kcp (h^{-1})	5.165	3.549	4.394
kpc (h^{-1})	16.949	21.090	9.552
V_{brain} (liters)	49.364	49.096	21.556
Kgmax-eye ($\log_{10}$ CFU/g/h)	0.080	0.070	0.029
Hg-eye	3.331	4.958	2.010
$C_{50}g$-eye (mg/liter)	0.193	0.148	0.170
POPMAX-eye (CFU/g)	82,291	99,139	33,087
Kkmax-eye ($\log_{10}$ CFU/g/h)	0.651	0.380	0.623
Hk-eye	3.496	3.292	1.481
$C_{50}k$-eye (mg/liter)	0.710	0.687	0.291
Kgmax-kidney ($\log_{10}$ CFU/g/h)	0.096	0.092	0.0282
Hg-kidney	4.258	4.951	1.325
$C_{50}g$-kidney (mg/liter)	3.204	1.550	3.936
POPMAX-kidney (CFU/g)	49,984,300	84,269,040	47,137,700
Kkmax-kidney ($\log_{10}$ CFU/g/h)	0.563	0.585	0.207
Hk-kidney	3.018	4.064	1.481
$C_{50}k$-kidney (mg/liter)	15.309	18.701	7.286
Initial condition-eye (CFU/g)	3	3	2
Initial condition-kidney (CFU/g)	1,061	573	1,036

[a] SCL, clearance of anidulafungin from the central compartment; V_c and V_{eye}, volumes of central compartment and vitreous humor, respectively; kcp, kpc, kce, and kec, first-order rate constants that connect the respective compartments; *N*, burden (organisms/gram vitreous humor or kidney) of *Candida albicans*, Kgmax, maximal rate of growth in the vitreous humor or kidney; POPMAX, theoretical maximal density within the vitreous humor or kidney; Hg, slope function for the suppression of growth in the vitreous humor or kidney; $C_{50}g$, concentration of drug producing half-maximal suppression of growth; Kkmax, maximal rate of kill in the vitreous humor or kidney; Hk, slope functions for the fungal kill in the vitreous humor or kidney; $C_{50}k$, concentration of drug in the vitreous humor or kidney where fungal kill is half maximal.

The fit of the mathematical model to the data was reasonable, with coefficients of determination for the linear regression of observed versus predicted values (r^2) for the concentrations of anidulafungin in the plasma, concentrations of anidulafungin in the vitreous humor, and fungal density in the vitreous humor all >0.65. The mathematical model was used to estimate the residual fungal burden in both the kidney and vitreous humor following the administration of various dosages of anidulafungin. The relationship between the plasma AUC and the fungal burden in the kidney and the vitreous humor is shown in Fig. 4. There was a progressive decline in the kidney burden with increasing AUC. Stasis was achieved in the kidney with a plasma AUC of approximately 100 (Fig. 3). In contrast, the antifungal effect in the eye was completely different, with a much slower reduction in fungal burden with increasing drug exposure, despite the fungal burden at the initiation of therapy being significantly lower. For the vitreous humor, stasis was achieved with a plasma AUC of approximately 270 (Fig. 3). The AUCs (mean ± standard deviation) for neonates and infants receiving a maintenance dose of 3 mg/kg and children receiving 1.5 mg/kg/day i.v. were 115.87 ± 57.71 and 99.50 ± 33.50, respectively (these estimates were obtained from previous

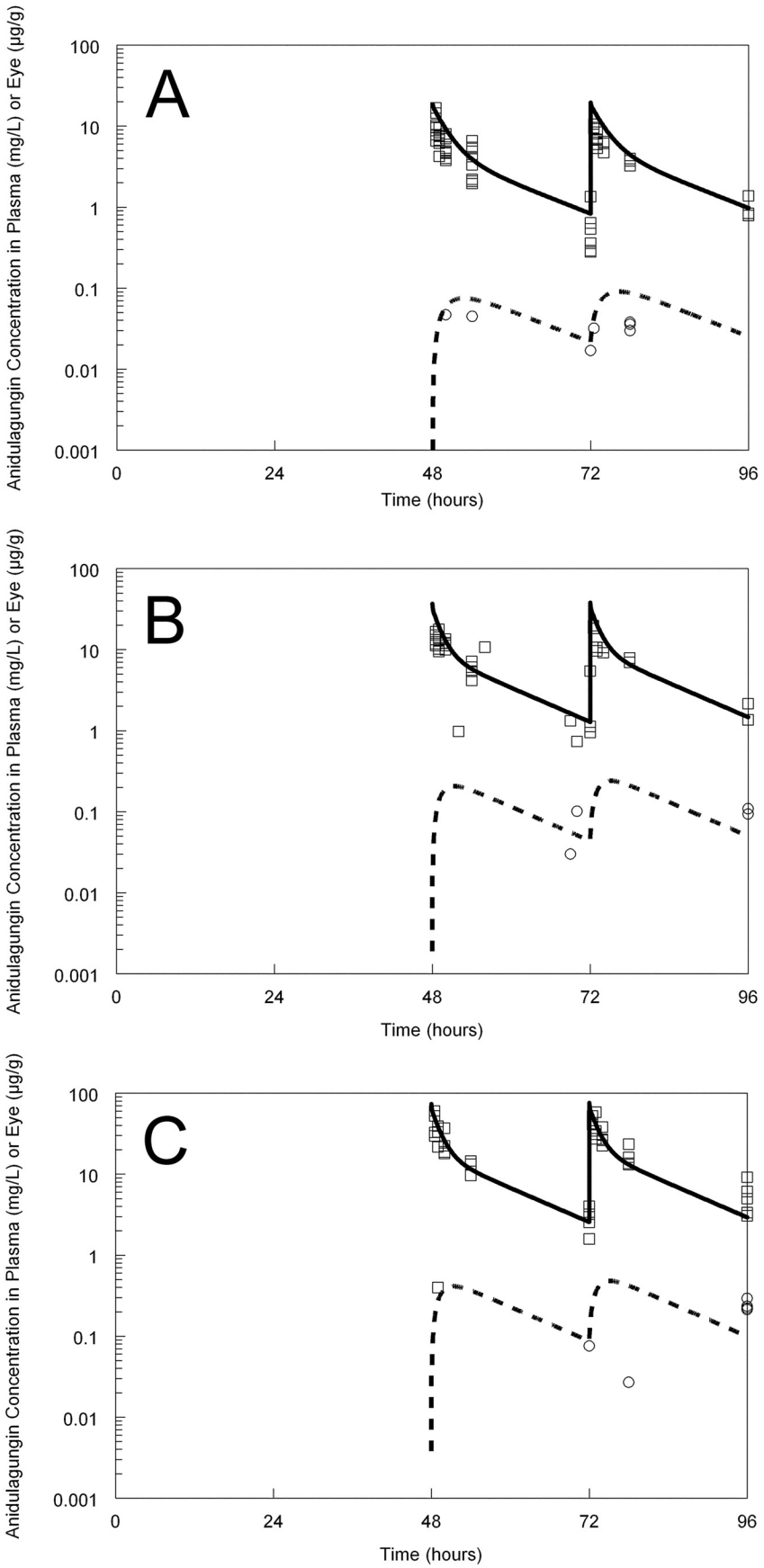

FIG 2 Pharmacokinetics of anidulafungin in the plasma (raw data shown by squares) and vitreous humor (raw data shown by circles). The dosage was 5 mg/kg (A), 10 mg/kg (B), or 20 mg/kg (C). The solid line is the fit of the mathematical model to the plasma data. The broken line is the fit of the mathematical model to the vitreous humor concentrations. Note that the plasma and tissue pharmacokinetics are shown on a semilogarithmic plot.

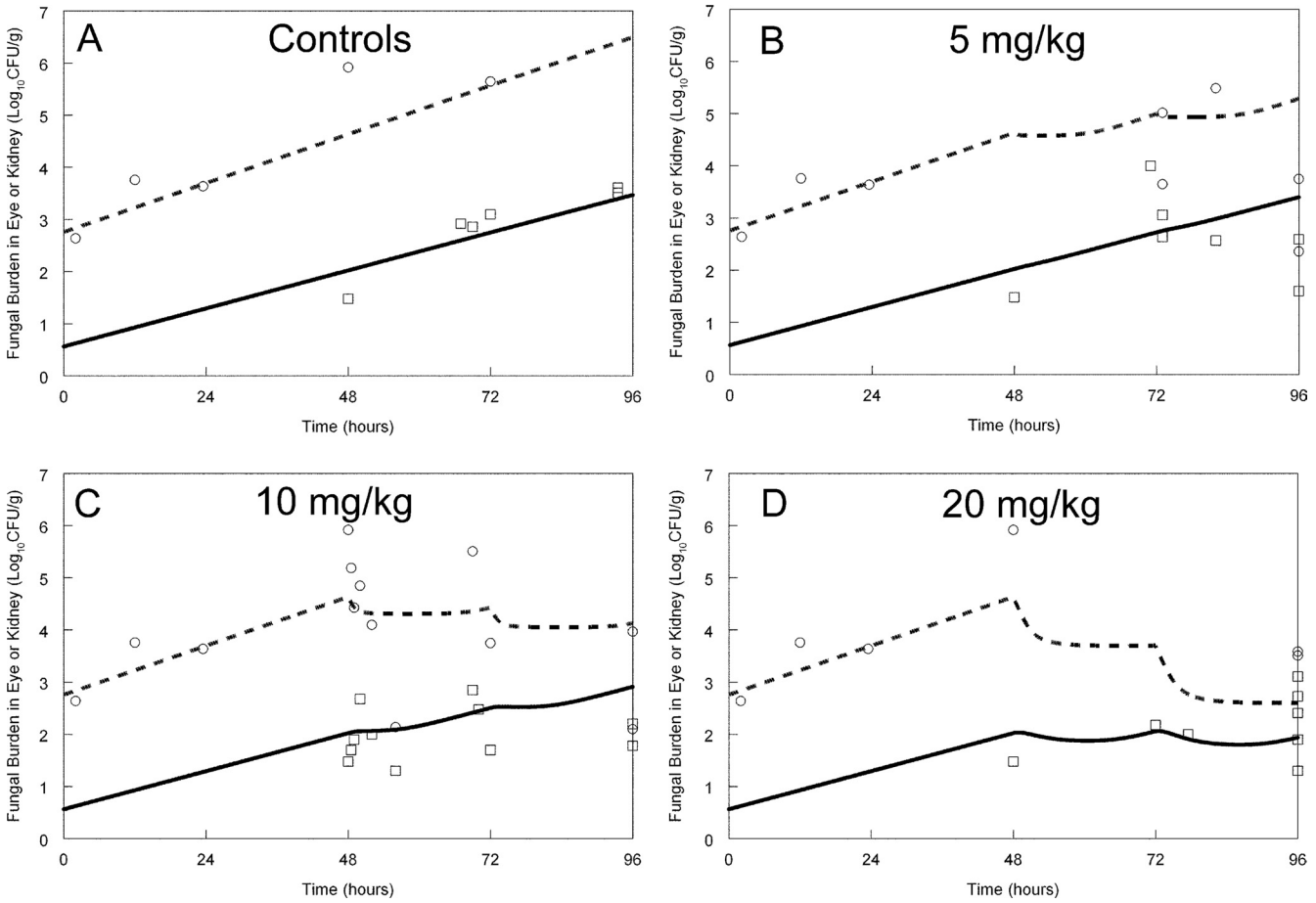

FIG 3 Pharmacodynamics of anidulafungin in the vitreous humor and the kidney. The raw data from the vitreous humor and kidney are shown by squares and circles, respectively. The fit of the mathematical model to the kidney data is shown by the broken line. The fit of the mathematical model to the vitreous humor data is shown by the solid line.

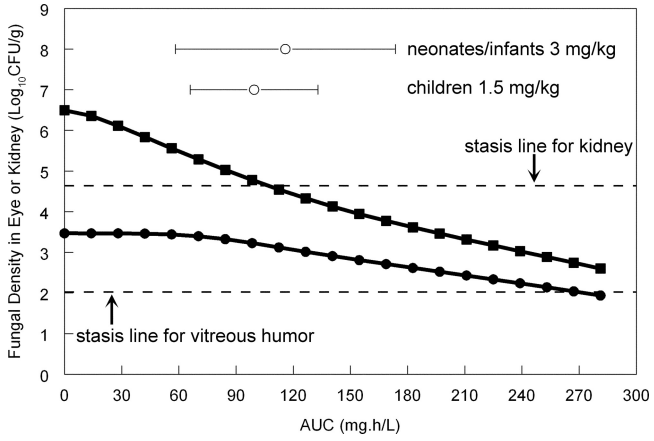

FIG 4 Simulations from the mathematical model relating the plasma area under the concentration-time curve (AUC) to residual fungal burden in the kidney (solid squares) or vitreous humor (solid circles) at the end of the experimental period. The stasis lines for the kidney and the vitreous humor are shown by the broken lines; these represent the fungal burden at the time that anidulafungin therapy is begun, 48 h after inoculation. The means ± standard deviations of the AUCs that develop in neonates/infants and children aged 2 to 17 are shown (open circles). An "average" adult patient receiving anidulafungin at 100 mg/day develops an AUC of approximately 105 mg · h/liter.

publications [16, 19]). A reasonable estimate for the mean AUC in adult patients receiving 100 mg per day is 105 mg · h/liter (calculated as dose [mg]/clearance [liters/h], or 100 mg/0.95 liter/h), but no robust estimates of dispersion are available. The AUCs for all three populations correspond to a fungistatic effect in the kidney but only minimal antifungal activity in the vitreous humor.

DISCUSSION

Candida endophthalmitis is a significant cause of morbidity for patients with disseminated candidiasis that can affect neonates, children, and adults. Estimates for the incidence of this syndrome range from 10 to 46% (20) in older studies to 1% in more recent studies (5). The reasons for the lower incidence in more recent studies are unknown but may potentially reflect more widespread use of antifungal prophylaxis.

As shown in Fig. 1, hematogenous dissemination of *Candida* spp. to the eye occurs via the long and short ciliary arteries (branches of the ophthalmic artery) and ultimately seeding of the highly vascular choroid (21). Fungal growth and invasion from this initial site lead to progressive involvement of the retinal pigment epithelium and retina; this syndrome is chorioretinitis and manifests clinically as fluffy white exudates on ophthalmoscopy. Further anterior extension into the vitreous humor leads to vitritis. Established infection of the vitreous and/or the aqueous hu-

mor of the anterior chamber constitutes the syndrome of *Candida* endophthalmitis. If untreated, widespread inflammation and necrosis occur, resulting in destruction of the globe and irreversible blindness. Acute symptoms are often initially floaters (mobile obscuration of vision), redness, and discomfort of the eye followed by visual loss. Visual impairment may result from retinal detachment, vitreous infiltration, central chorioretinal lesions (22), and/or cataract formation (23). Endogenous endophthalmitis is a particular threat to quality of life because of its propensity to cause bilateral visual loss.

The eye is a sanctuary site that is normally protected by the blood-ocular barrier, which performs a similar function to that of the blood-brain barrier. The blood-ocular barrier controls the transport of nutrients from the choroid to the retina and prevents the unrestricted transgression of xenobiotics. The blood-ocular barrier is comprised of two layers: an outer barrier and an inner barrier (24). The outer layer comprises retinal pigment epithelium that controls movement of molecules between the choroid and the retina. Paracellular molecular movement is limited by tight junctions between the apical aspects of the cells. The inner barrier comprises those elements that make up the walls of the retinal capillaries, principally the nonfenestrated endothelial cells bound by tight junctions supported by Muller cells and astrocytes (Fig. 1). Infection that is extraneous to the blood-ocular barrier may be successfully treated with systemic antifungal agents alone. Treatment of infections beyond the blood-ocular barrier is significantly complicated by poor penetration of many antifungal agents and therefore often requires adjunctive treatments such as vitrectomy and the intravitreal instillation of antifungal agents. The therapeutic implications of the blood-ocular barrier were readily apparent in this study, where the exposure-response relationships for anidulafungin in the vitreous humor and kidney were completely discordant. The AUCs for stasis in the eye and kidney were approximately 270 and 100 mg · h/liter, respectively.

In keeping with the other licensed echinocandins, anidulafungin is a large water-soluble lipopeptide with a molecular mass of approximately 1,200 Da (11). The mechanism of penetration of anidulafungin into the vitreous humor is unclear. The presence of an echinocandin transporter is possible but has not been described. Alternatively, disruption of the blood-ocular barrier by the pathological process may facilitate drug penetration, and this has been previously described for fluconazole, itraconazole, and ketoconazole in experimental *Candida* endophthalmitis (15). Regardless of the transport mechanism(s), we demonstrated quantifiable anidulafungin concentrations in the vitreous humor in the first dosing interval. Although the total drug exposure, quantified in terms of the AUC, was only a small fraction of that in plasma (2.3%), we were able to demonstrate clear antifungal activity. In this regard, the results are reminiscent of those for compounds such as itraconazole, where the intraocular concentrations are relatively low but there is an antifungal effect that is comparable to those of agents such as fluconazole that readily penetrate the eye (15).

Despite considerable evidence to the contrary (see, for example, references 14, 25, and 26), the echinocandins are consistently reported to be compounds that do not penetrate the eye or other parts of the central nervous system and agents that should not be used to treat fungal infections at these sites. The clinical outcomes for patients with endophthalmitis receiving echinocandins are variable (27–30). Progressive endophthalmitis has been attributed to poor ocular penetration of caspofungin (28). Our study suggests that anidulafungin may be an effective agent for the treatment of *Candida* endophthalmitis but only at significantly higher dosages than are currently licensed or commonly used. For an example, an "average" adult healthy volunteer receiving anidulafungin at 100 mg/day develops an AUC of approximately 105 mg · h/liter (100 mg divided by 0.95 liter/h) (19). There are currently no published population pharmacokinetic models for patients that provide an estimate of the range of AUCs that develop with standard dosing. An AUC of approximately 100 mg · h/liter is associated with significant antifungal activity in the kidney (attainment of stasis and ~2 log units of effect) (Fig. 3 and 4) but relatively minimal antifungal activity in the eye (Fig. 3 and 4). As further shown in Fig. 4, an AUC of approximately 270 mg · h/liter is required to achieve stasis in the eye, which (assuming linear pharmacokinetics with dosage escalation) would require approximately 250 to 300 mg/day in adults. Similar dosage escalation would also be required for neonates and children. At the current time, there are no pharmacokinetic data or models for these higher dosages in any age group. In contrast, both caspofungin and micafungin have been studied at higher dosages than are routinely used in clinical practice (31–33). Certainly, the wide therapeutic index that is characteristic of the echinocandins suggests that use of higher dosages of anidulafungin may be possible.

There are a number of limitations and assumptions in this study. First, we studied only a single strain of *Candida albicans*, and there are strain-to-strain differences in the invasive potential and therefore the pharmacodynamic relationships of anidulafungin against *Candida* in the eye. Second, we did not consider the implication of combined surgical therapy (vitrectomy) or of anidulafungin in combination with other antifungal agents. Third, the validity of the bridging study is based on the assumption that the rates and extents of trafficking of anidulafungin from the plasma to the vitreous humor in rabbits and humans are comparable. Despite these potential limitations, the model is a rigorous test of antifungal activity primarily because of the treatment delay of 48 h, which enables infection and invasion to become well established before treatment is initiated. We have demonstrated that anidulafungin does penetrate the eye and that the achievement of significant antifungal activity requires higher dosages than are currently used. Therefore, this study provides the experimental foundation for the appropriate use of anidulafungin for ocular infections. Well-designed pharmacokinetic-pharmacodynamic studies in laboratory animal models and patients represent an efficient way in which antifungal therapy for *Candida* endophthalmitis can be further optimized.

ACKNOWLEDGMENTS

W. W. Hope is supported by a National Institute of Health Research (NIHR) Clinician Scientist Award. T. W. Felton is supported by a Medical Research Council (MRC) Clinical Pharmacology Fellowship. This work was supported in part by Pfizer Inc.

The schematic figures of the eye were drawn by Angela Luck.

W. W. Hope has given talks, received research grants, and served as a consultant to Pfizer.

REFERENCES

1. **Benjamin DK, Jr, Poole C, Steinbach WJ, Rowen JL, Walsh TJ.** 2003. Neonatal candidemia and end-organ damage: a critical appraisal of the literature using meta-analytic techniques. Pediatrics **112**:634–640.
2. **Donahue SP, Hein E, Sinatra RB.** 2003. Ocular involvement in children with candidemia. Am. J. Ophthalmol. **135**:886–887.

3. **Rodriguez D, Almirante B, Park BJ, Cuenca-Estrella M, Planes AM, Sanchez F, Gene A, Xercavins M, Fontanals D, Rodriguez-Tudela JL, Warnock DW, Pahissa A.** 2006. Candidemia in neonatal intensive care units: Barcelona, Spain. Pediatr. Infect. Dis. J. **25**:224–229.
4. **Speer ME, Hittner HM, Rudolph AJ.** 1980. *Candida* endophthalmitis: a manifestation of candidiasis in the neonate. South Med. J. **73**:1407–1409.
5. **Dozier CC, Tarantola RM, Jiramongkolchai K, Donahue SP.** 2011. Fungal eye disease at a tertiary care center: the utility of routine inpatient consultation. Ophthalmology **118**:1671–1676.
6. **Huynh N, Chang HY, Borboli-Gerogiannis S.** 2012. Ocular involvement in hospitalized patients with candidemia: analysis at a Boston tertiary care center. Ocul Immunol. Inflamm. **20**:100–103.
7. **Shah CP, McKey J, Spirn MJ, Maguire J.** 2008. Ocular candidiasis: a review. Br. J. Ophthalmol. **92**:466–468.
8. **Pappas PG, Kauffman CA, Andes D, Benjamin DK, Jr, Calandra TF, Edwards JE, Jr, Filler SG, Fisher JF, Kullberg BJ, Ostrosky-Zeichner L, Reboli AC, Rex JH, Walsh TJ, Sobel JD.** 2009. Clinical practice guidelines for the management of candidiasis: 2009 update by the Infectious Diseases Society of America. Clin. Infect. Dis. **48**:503–535.
9. **Varma D, Thaker HR, Moss PJ, Wedgwood K, Innes JR.** 2005. Use of voriconazole in candida retinitis. Eye (Lond) **19**:485–487.
10. **Akler ME, Vellend H, McNeely DM, Walmsley SL, Gold WL.** 1995. Use of fluconazole in the treatment of candidal endophthalmitis. Clin. Infect. Dis. **20**:657–664.
11. **Denning DW, Hope WW.** 2010. Therapy for fungal diseases: opportunities and priorities. Trends Microbiol. **18**:195–204.
12. **Reboli AC, Rotstein C, Pappas PG, Chapman SW, Kett DH, Kumar D, Betts R, Wible M, Goldstein BP, Schranz J, Krause DS, Walsh TJ.** 2007. Anidulafungin versus fluconazole for invasive candidiasis. N. Engl. J. Med. **356**:2472–2482.
13. **Groll AH, Giri N, Petraitis V, Petraitiene R, Candelario M, Bacher JS, Piscitelli SC, Walsh TJ.** 2000. Comparative efficacy and distribution of lipid formulations of amphotericin B in experimental Candida albicans infection of the central nervous system. J. Infect. Dis. **182**:274–282.
14. **Hope WW, Mickiene D, Petraitis V, Petraitiene R, Kelaher AM, Hughes JE, Cotton MP, Bacher J, Keirns JJ, Buell D, Heresi G, Benjamin DK, Jr, Groll AH, Drusano GL, Walsh TJ.** 2008. The pharmacokinetics and pharmacodynamics of micafungin in experimental hematogenous *Candida* meningoencephalitis: implications for echinocandin therapy in neonates. J. Infect. Dis. **197**:163–171.
15. **Savani DV, Perfect JR, Cobo LM, Durack DT.** 1987. Penetration of new azole compounds into the eye and efficacy in experimental *Candida* endophthalmitis. Antimicrob. Agents Chemother. **31**:6–10.
16. **Warn PA, Livermore J, Howard S, Felton TW, Sharp A, Gregson L, Goodwin J, Petraitiene R, Petraitis V, Cohen-Wolkowiez M, Walsh TJ, Benjamin DK, Jr, Hope WW.** 2012. Anidulafungin for neonatal hematogenous *Candida* meningoencephalitis: identification of candidate regimens for humans using a translational pharmacological approach. Antimicrob. Agents Chemother. **56**:708–714.
17. **Leary R, Jelliffe R, Schumitzky A, van Guilder M.** 2001. An adaptive grid, non-parametric approach to pharmacokinetic and dynamic (PK/PD) models, p 389–394. Proceedings, Fourteenth IEEE Computer Society. IEEE Computer Society, Bethesda MD.
18. **D'Argenio DZ, Schumitzky A, Wang X.** 2009. ADAPT 5 user's guide: pharmacokinetic/pharmacodynamic systems analysis software. Biomedical Simulations Resource, Los Angeles, CA.
19. **Dowell JA, Knebel W, Ludden T, Stogniew M, Krause D, Henkel T.** 2004. Population pharmacokinetic analysis of anidulafungin, an echinocandin antifungal. J. Clin. Pharmacol. **44**:590–598.
20. **McDonnell PJ, McDonnell JM, Brown RH, Green WR.** 1985. Ocular involvement in patients with fungal infections. Ophthalmology **92**:706–709.
21. **Omuta J, Uchida K, Yamaguchi H, Shibuya K.** 2007. Histopathological study on experimental endophthalmitis induced by bloodstream infection with *Candida albicans.* Jpn. J. Infect. Dis. **60**:33–39.
22. **Sallam A, Taylor SR, Khan A, McCluskey P, Lynn WA, Manku K, Pacheco PA, Lightman S.** 2012. Factors determining visual outcome in endogenous *Candida* endophthalmitis. Retina **32**:1129–1134.
23. **Clinch TE, Duker JS, Eagle RC, Jr, Calhoun JH, Augsburger JJ, Fischer DH.** 1989. Infantile endogenous Candida endophthalmitis presenting as a cataract. Surv. Ophthalmol. **34**:107–112.
24. **Kaur C, Sivakumar V, Yong Z, Lu J, Foulds WS, Ling EA.** 2007. Blood-retinal barrier disruption and ultrastructural changes in the hypoxic retina in adult rats: the beneficial effect of melatonin administration. J. Pathol. **212**:429–439.
25. **Petraitis V, Petraitiene R, Groll AH, Roussillon K, Hemmings M, Lyman CA, Sein T, Bacher J, Bekersky I, Walsh TJ.** 2002. Comparative antifungal activities and plasma pharmacokinetics of micafungin (FK463) against disseminated candidiasis and invasive pulmonary aspergillosis in persistently neutropenic rabbits. Antimicrob. Agents Chemother. **46**:1857–1869.
26. **Suzuki T, Uno T, Chen G, Ohashi Y.** 2008. Ocular distribution of intravenously administered micafungin in rabbits. J. Infect. Chemother. **14**:204–207.
27. **Breit SM, Hariprasad SM, Mieler WF, Shah GK, Mills MD, Grand MG.** 2005. Management of endogenous fungal endophthalmitis with voriconazole and caspofungin. Am. J. Ophthalmol. **139**:135–140.
28. **Gauthier GM, Nork TM, Prince R, Andes D.** 2005. Subtherapeutic ocular penetration of caspofungin and associated treatment failure in Candida albicans endophthalmitis. Clin. Infect. Dis. **41**:e27–28.
29. **Mousselli HA, Norwood J.** 2012. Failure of echinocandin therapy in the treatment of Candida glabrata chorioretinitis. Am. J. Med. Sci. **343**:98–100.
30. **Sarria JC, Bradley JC, Habash R, Mitchell KT, Kimbrough RC, Vidal AM.** 2005. *Candida glabrata* endophthalmitis treated successfully with caspofungin. Clin. Infect. Dis. **40**:e46–48.
31. **Betts RF, Nucci M, Talwar D, Gareca M, Queiroz-Telles F, Bedimo RJ, Herbrecht R, Ruiz-Palacios G, Young JA, Baddley JW, Strohmaier KM, Tucker KA, Taylor AF, Kartsonis NA.** 2009. A multicenter, double-blind trial of a high-dose caspofungin treatment regimen versus a standard caspofungin treatment regimen for adult patients with invasive candidiasis. Clin. Infect. Dis. **48**:1676–1684.
32. **Pappas PG, Rotstein CM, Betts RF, Nucci M, Talwar D, De Waele JJ, Vazquez JA, Dupont BF, Horn DL, Ostrosky-Zeichner L, Reboli AC, Suh B, Digumarti R, Wu C, Kovanda LL, Arnold LJ, Buell DN.** 2007. Micafungin versus caspofungin for treatment of candidemia and other forms of invasive candidiasis. Clin. Infect. Dis. **45**:883–893.
33. **Sirohi B, Powles RL, Chopra R, Russell N, Byrne JL, Prentice HG, Potter M, Koblinger S.** 2006. A study to determine the safety profile and maximum tolerated dose of micafungin (FK463) in patients undergoing haematopoietic stem cell transplantation. Bone Marrow Transplant. **38**:47–51.